

Hypoxia and tissue destruction in pulmonary tuberculosis

Moerida Belton¹, Sara Brilha¹, Roido Manavaki², Francesco Mauri³, Kuldip Nijran⁴, Young T. Hong⁵, Neva H. Patel⁴, Marcin Dembek¹, Liku Tezera⁶, Justin Green¹, Rachel Moores¹, Franklin Aigbirhio⁵, Adil Al-Nahhas⁴, Tim D. Fryer⁵, Paul T. Elkington^{1,6}, Jon S. Friedland¹

¹ Section of Infectious Diseases and Immunity, Imperial College London, UK

² Department of Radiology, School of Clinical Medicine, University of Cambridge, UK

³ Department of Histopathology, Hammersmith Campus, Imperial College London, UK

⁴ Radiological Science Unit Charing Cross Campus, Department of Nuclear Medicine, Charing Cross Campus, Imperial College NHS Trust, London, UK

⁵ Wolfson Brain Imaging Centre, School of Clinical Medicine, University of Cambridge, UK

⁶ NIHR Respiratory Biomedical Research Unit, Faculty of Medicine, University of Southampton, UK

Corresponding author: Jon S Friedland
Section of Infectious Diseases and Immunity
Du Cane Road, London W12 0NN
United Kingdom
E-mail: j.friedland@imperial.ac.uk
Tel: 44 (0)20 8383 8521 Fax: 44 (0)20 8383 3394

Key words: Tuberculosis, hypoxia, HIF-1 α , MMP-1

Word Count 2,997

ABSTRACT

Background: It is unknown whether lesions in human tuberculosis (TB) are hypoxic or whether this influences disease pathology. Human TB is characterized by extensive lung destruction driven by host MMPs, particularly collagenases such as MMP-1.

Methods: We investigated tissue hypoxia in five patients with PET imaging using the tracer [^{18}F]-fluoromisonidazole ([^{18}F]FMISO) and by immunohistochemistry. We studied regulation of MMP secretion in primary human cell culture model systems in normoxia, hypoxia, chemical hypoxia and by siRNA inhibition.

Results: [^{18}F]FMISO accumulated in regions of TB consolidation and around pulmonary cavities, demonstrating for the first time severe tissue hypoxia in man. Patlak analysis of dynamic PET data showed heterogeneous levels of hypoxia within and between patients. In *Mycobacterium tuberculosis* (*M.tb*)-infected human macrophages, hypoxia (1% pO₂) upregulated MMP-1 gene expression 170-fold, driving secretion and caseinolytic activity. Dimethyloxalyl glycine, a small molecule inhibitor which stabilises the transcription factor Hypoxia Inducible Factor (HIF)-1 α , similarly upregulated MMP-1. Hypoxia did not affect mycobacterial replication. Hypoxia increased MMP-1 expression in primary respiratory epithelial cells via intercellular networks regulated by TB. HIF-1 α and NF- κ B regulated increased MMP-1 activity in hypoxia. Furthermore, *M.tb* infection drove HIF-1 α accumulation even in normoxia. In human TB lung biopsies, epithelioid macrophages and multi-nucleate giant cells express HIF-1 α . HIF-1 α blockade including by targeted siRNA inhibited TB-driven MMP-1 gene expression and secretion.

Conclusions: Human TB lesions are severely hypoxic and *M.tb* drives HIF- 1 α accumulation, synergistically increasing collagenase activity which will lead to lung destruction and cavitation

What is the key question?

Is there functionally important hypoxia within human pulmonary TB lesions?

What is the bottom line?

Human TB lesions are severely hypoxic, and hypoxia exacerbates matrix metalloproteinase-mediated inflammatory tissue destruction.

Why read on?

This study uses PET-CT to demonstrate for the first time that human lung lesions are severely hypoxic and demonstrates that hypoxia, at the level seen in humans, potentially upregulates matrix metalloproteinase-1, a collagenase central to both cavity formation and spread of infection.

INTRODUCTION

Mycobacterium tuberculosis (*M.tb*) is solely a pathogen of humans and infects one third of the global population, killing 1.5 million people each year [1]. Drug resistance in tuberculosis is increasing and there relatively few new drugs on the horizon. Novel approaches to therapy require an understanding of the immune-pathology of TB. Lung tissue destruction is a hallmark of pulmonary tuberculosis (TB) [2] and is key for transmission of infection. Reduced tissue oxygenation has been noted in animal models of TB [3, 4], but hypoxia in human disease has not been investigated although may have a significant effect on the host response. The pathology of human TB is different to most animal models [2]. Furthermore, although extensive lung damage is found in TB, the effect of hypoxia on proinflammatory tissue destruction in TB has not been explored.

MMPs are emerging as key proteases causing TB immunopathology. Recent evidence implicates MMPs, particularly collagenases such as MMP-1, as key in driving tissue destruction during pulmonary TB [5-7]. Since MMPs may cause uncontrolled proteolytic destruction, MMP activity is tightly regulated at the transcriptional level, by cleavage of the proenzyme to an active form and by specific Tissue Inhibitors of Metalloproteinases (TIMPs) which negatively regulate protease activity. Regulation of MMPs by hypoxia in TB has not been studied.

The cellular response to hypoxia is orchestrated by HIF-1, a heterodimeric transcription factor considered a master regulator of the host response to oxygen deprivation [8, 9]. In addition to regulating oxygen homeostasis, emerging evidence implicates HIF-1 in infectious

and inflammatory diseases [10]. HIF-1 is comprised of two subunits; oxygen-responsive HIF-1 α and constitutively expressed HIF-1 β . In normoxia, HIF-1 α is hydroxylated by prolyl-4-hydroxylase proteins (PHDs) [11, 12], allowing binding of the von Hippel-Lindau protein which targets HIF-1 α for proteosomal degradation [13]. Under hypoxic conditions PHD activity declines, resulting in HIF-1 α accumulation and HIF-1 heterodimer stabilization [14]. This HIF-1 complex binds to promoter regions of hypoxia-inducible genes, upregulating an array of genes including those involved in cell survival, angiogenesis, apoptosis, erythropoiesis, glucose metabolism and pH regulation [11]. HIF is responsive to a variety of stimuli, with the inflammatory transcription factor NF- κ B being of particular importance in modulation of HIF expression [9]. The complex interaction between HIF-1 α and NF- κ B signifies a synergistic link between hypoxia and immune responses, indicating a potential role of hypoxia in driving TB immunopathology.

In this study, we show for the first time that lesions in pulmonary TB infection are severely hypoxic in man. There is heterogeneity both within and between lesions in the extent of hypoxia. In primary human monocyte-derived macrophages (MDMs) and normal human bronchial epithelial cells (NHBEs), hypoxia synergistically upregulates HIF-1 α -dependent MMP-1 (collagenase) gene expression and secretion during *M.tb* infection. In addition, *M.tb* stabilizes HIF-1 α even in the absence of hypoxia. HIF-1 α accumulation is necessary for MMP-1 secretion and HIF-1 α is highly expressed in macrophages in human TB granulomas.

METHODS

Full methods are provided in the online supplement.

Patient Recruitment

Ethical approval for the study was obtained from East London and City Research Ethics Committee and Imperial College Healthcare Trust Joint Research Office, with further approval by the UK Administration of Radioactive Substances Advisory Committee (ARSAC). Patients were recruited from Imperial College Healthcare NHS Trust with a confirmed microbiological diagnosis of TB, either on acid-fast smear and / or *M.tb* culture. All patients had abnormal plain chest radiographs and had received less than 2 weeks of anti-TB therapy. Informed consent was obtained from all study participants.

¹⁸F-MISO PET-CT scans

PET-CT scans were performed on a Siemens mCT (Siemens Medical, Erlangen, Germany) at the Department of Nuclear Medicine Charing Cross Hospital, Imperial College NHS Trust, London. [¹⁸F]FMISO was synthesized in the Wolfson Brain Imaging Centre, University of Cambridge. Patient scanning protocol and data analysis are described in the online supplement.

***M.tb* culture**

M.tuberculosis H375v was cultured in Middlebrook 7H9 medium as previously described [15].

Cell Culture Experiments

Monocyte-derived primary human macrophages were infected with *M.tb* H37Rv as described [15]. Primary human bronchial epithelial cells (Lonza, Slough, UK) were cultured and stimulated with conditioned media from *Mtb*-infected monocytes (CoMtb) and A549 cells transiently transfected as described [16].

Hypoxia workstation

A custom designed hypoxia workstation was commissioned for the biological safety level 3 facility (Coy Laboratories, USA).

Casein Zymography

Casein zymography was performed as previously described [15].

Real-time PCR

Macrophages were lysed using Tri-Reagent (Sigma-Aldrich, Dorset, UK), and total RNA was extracted using PureLink RNA[®] Mini Kit (Invitrogen, Paisley, UK). RNA was reverse transcribed using QuantiTect Reverse Transcriptase Kit (Qiagen, Manchester, UK). qPCR reactions were performed in an ABI Prism 7700 (Applied Biosystems, Paisley, UK).

Measurement of MMP and TIMP concentrations

Total MMP and TIMP secretion in cell culture supernatants was measured by ELISA (R&D Systems, Abdingdon, UK) or on the Luminex 200 platform using MMP Luminex multiplex array (R&D Systems, Abingdon, UK) according to the manufacturer's instructions. The minimum level of detection for MMP-1 was 10 pg/ml.

HIF-1 α Western analysis

Western blotting was performed using anti-HIF1 α Ab (BD Biosciences, UK) and goat anti-mouse IgG horseradish peroxidase (HRP)-conjugate secondary Ab (Jackson ImmunoResearch). Loading control was performed using the rabbit-anti β -actin Ab and goat anti-mouse IgG horseradish peroxidase (HRP)-conjugate secondary Ab (Jackson ImmunoResearch). Luminescence was detected with the ECL system (Amersham, UK) according to manufacturer's protocol.

Confocal microscopy

Primary human monocyte-derived macrophages were infected with *M.tb* H37RV in Permanox plastic chamber slides (Thermo Fisher Scientific Inc. UK). MMP-1 staining was performed using anti-MMP-1 primary Ab (Abcam, UK) and goat anti-mouse secondary Ab (Abcam, UK) according to the manufacturers' instructions. Nuclei were visualized using DAPI.

SiRNA

MDMs were transfected using DharmaFECT 3 transfection reagent with either non-targeting control siRNA or HIF-1 α siRNA smartpool (Dharmacon, FisherScientific, Loughborough, UK), according to the supplier's instructions.

Immunohistochemistry

HIF-1 α immunohistochemistry was performed on formalin-fixed, paraffin-embedded lung biopsies from six patients with culture-proved *M.tb* infection and six non-infected control samples. Immunohistochemistry staining was performed using Bond III fully automated

staining system with the Bond Polymer Refine Detection system and associated reagents (Leica Microsystems, Newcastle-Upon-Tyne, UK). HIF-1 α was detected using HIF1- α antibody (Abcam AB1).

Statistics

Statistical analysis was performed using GraphPad PRISM 6. Data was analyzed with Kruskal-Wallis for comparison between 3 or more groups and Dunn's test for pairwise comparisons. A *P* value of 0.05 was considered significant. For all experiments, bars represent mean values \pm SD from a minimum of two independent experiments performed in triplicate.

RESULTS

Regions of severe hypoxia are present in human pulmonary TB lesions

To investigate hypoxia in TB patients, we performed PET-CT scans in patients who had acid-fast bacilli identified in respiratory specimens that were subsequently culture confirmed to be *M.tb* (Patient demographics and microbiology are in Supplementary table 1). The average duration of pulmonary symptoms was 2.4 months and all patients were HIV negative (Patient laboratory data are presented in Supplementary table 2). To investigate hypoxia, we used the hypoxia-specific tracer ^{18}F -fluoromisonidazole (^{18}F FMISO), which has been used to study tumour biology [17]. ^{18}F FMISO is selectively trapped in severely hypoxic regions ($\text{pO}_2 < 10\text{mmHg}$) [18-20]. PET-CT scans in 5 patients demonstrated extensive uptake of ^{18}F FMISO in radiologically abnormal areas of the lung, as assessed by ^{18}F FMISO target-to-background (TBR) (Figure 1A), with the lateral muscle used as a background representing normoxic tissue. TBR values significantly greater than unity were found in one or more lesions in all patients (Figure 1B).

To provide a more specific measure of hypoxia than TBR, Patlak K_i mapping was applied, which demonstrated the presence of severe hypoxia within areas of consolidation and in the regions immediately surrounding pulmonary cavities (Figure 2A and Supplementary Table 3). All patients had K_i values greater than a hypoxia threshold in at least one region of interest (Figure 2B). Heterogeneous levels of hypoxia were seen within patients with the exception of Patient 2, who demonstrated evidence of severe hypoxia in all ROIs. Finally, time-activity curves demonstrated significantly higher levels of ^{18}F FMISO within ROIs compared to peripheral blood (Figure 2C). Together, these data demonstrate for the first time the presence of severe hypoxia within TB lesions in man.

Hypoxia increases *M.tb*-driven MMP-1 expression in human macrophages

Next, the effect of hypoxia (1% pO₂) on gene expression and secretion of MMP-1 was investigated. Hypoxia significantly increased MMP-1 gene expression in *M.tb*-infected human MDMs compared to infection in normoxia (21% pO₂), resulting in a 170-fold increase in MMP-1 mRNA accumulation at 24h (Figure 3A, $p < 0.0001$ by Kruskal-Wallis test). Increased MMP-1 accumulation under hypoxic conditions in *M.tb*-infected MDMs was confirmed by confocal microscopy (Figure 3B). In both normoxia and hypoxia, *M.tb* was a more potent stimulus to MMP-1 secretion than LPS (Figure 3C, $p < 0.05$ and $p < 0.01$ respectively). Casein zymography demonstrated that the increased MMP-1 secretion in hypoxia was proteolytically active (Figure 3D).

Next, we used dimethyloxalyl glycine (DMOG) to block prolyl hydroxylase activity, thereby stabilizing HIF-1 α and activating the HIF-1 pathway. Consistent with findings in 1% pO₂, DMOG significantly increased MMP-1 secretion in *M.tb*-infected macrophages, causing a dose-dependent increase in secretion and caseinolytic activity (Figure 3E). Hypoxia caused no difference in *M.tb* colony forming units 72 hrs post infection (data not shown), demonstrating that intracellular replication of *M.tb* was not altered.

Hypoxia increases *M.tb*-dependent MMP-1 expression in respiratory epithelial cells

Next, we investigated the effect of hypoxia on respiratory epithelial cell MMP-1 secretion, as stromal cell networks are important sources of MMPs in TB [16]. Conditioned media from *M.tb*-infected monocytes (CoMTb) stimulation of primary NHBs in hypoxia (5% and 1% pO₂) increased MMP-1 secretion (Figure 4A; $p < 0.05$). LDH release assay showed that

hypoxia did not increase cell cytotoxicity (Supplementary Figure 1). Such MMP-1 secretion is potentially open to modification by small molecules, since stabilization of HIF-1 α by DMOG also increased MMP-1 secretion in CoMTb-stimulated NHBEs in a dose-dependent manner (Figure 4B, $p<0.01$). In addition, 0.25mM DMOG increased NHBE cell MMP-9 secretion and proteolytic activity on gelatin zymography (Supplementary Figure 2).

There were similar findings in the A549 respiratory epithelial cell line (Supplementary Figure 3). *In silico* analysis of the MMP-1 promoter sequence demonstrated numerous putative hypoxia response elements (HREs) which are HIF-1 binding sites, as well as known NF- κ B and AP-1 binding sites (Figure 4C). A549 cells were transiently transfected with either full length MMP-1 promoter-reporter genes or truncation constructs and stimulated with CoMTb in the presence or absence of hypoxia. In normoxia, deletions upstream of -2941 resulted in increased MMP-1 promoter activity indicating the presence of inhibitory elements (Figure 4D). Deletions downstream of -2941bp from the transcriptional start site reduced MMP-1 promoter activity. The presence of hypoxia resulted in increased MMP-1 promoter activity, compared to normoxia, in deletion constructs upstream of -1551. To investigate whether NF- κ B regulated MMP-1 expression in hypoxia, IKK- β activity was inhibited by SC-514. IKK- β inhibition significantly decreased MMP-1 secretion in a dose-dependent manner in normoxia and this effect was more pronounced in hypoxia (Figure 4E). Site-directed mutagenesis of the NF- κ B binding site between -2878 and -2886 bp in the MMP-1 promoter reduced MMP-1 promoter activity observed in hypoxia (Figure 4H; $p<0.01$ by Kruskal-Wallis).

M.tb stabilizes HIF-1 α , driving MMP-1 expression, and HIF-1 α is expressed in TB patient granulomas

Next, we investigated whether *M.tb* directly affected HIF-1 α accumulation independently of the stimulus from hypoxia. In respiratory epithelial cells, DMOG and CoMTb-stimulation of A549 cells independently upregulated HIF-1 α . Concurrent exposure to DMOG and stimulation by CoMTb resulted in maximal accumulation of HIF-1 α (Figure 5A). In human MDMs, *M.tb* infection in normoxia induced stabilization and accumulation of HIF-1 α peaking at 24 hours (Figure 5B). Hypoxia and *M.tb* infection synergistically drove prolonged and increased HIF-1 α accumulation in MDMs compared to cells exposed to either stimulus alone, with HIF-1 α accumulation detectable from 4 hours after infection (Figure 5C). *M.tb* infection did not induce HIF-2 accumulation either in normoxia or hypoxia (data not shown).

To investigate whether HIF-1 α regulated MMP-1 expression during TB infection, we inhibited the activity of HIF-1 α in normoxia and hypoxia. The inhibitor LW6 caused a trend to decreased *M.tb*-driven MMP-1 secretion in human MDMs in normoxia, but in hypoxia there was a significant dose-dependent decrease in MMP-1 secretion (Figure 5D; $p < 0.05$). To confirm this observation, further studies were performed with HIF-1 α siRNA. Western blot analysis demonstrated that targeted but not non-targeting siRNA decreased HIF-1 α protein in *M.tb* infected MDMs in normoxia and hypoxia (Figure 6A). HIF-1 α siRNA decreased MMP-1 mRNA accumulation (Figure 6B; $p < 0.0001$) and protein secretion (Figure 6C) in both normoxic and hypoxic conditions ($p < 0.05$). Non-targeted siRNA did not suppress MMP-1 gene expression or protein secretion.

To investigate the relevance of HIF-1 α to TB granulomas in patients, we performed immunohistochemical analysis of lung biopsy specimens from patients with a confirmed

diagnosis of TB. Epithelioid macrophages and Langerhans giant cells were immunoreactive for HIF-1 α staining within TB granulomas (Figure 6D i,ii) compared to uninfected control lung tissue (Figure 6D iii), demonstrating that TB infection causes HIF-1 α accumulation.

DISCUSSION

In this first detailed study of hypoxia in human tuberculosis, we demonstrate the presence of severe hypoxia within areas of lung consolidation and around pulmonary cavities in human TB. Hypoxia increases gene expression and secretion of MMP-1, a key collagenase that causes tissue destruction and immunopathology in pulmonary TB. In addition, *M.tb* infection directly drives HIF-1 α accumulation, which is further increased in hypoxia to synergistically activate immunopathogenic signalling pathways.

We demonstrated hypoxia in human TB using [^{18}F]FMISO PET-CT scanning for the first time in patients with an infectious disease. Hypoxia has not previously been found in man although reported in animal models of TB, all of which have somewhat different pathology to human disease [3, 4]. Until now, the investigation of hypoxia and TB has focussed primarily on pathogen responses to oxygen restriction, controlled by the two-component regulation system dosR/dosS (or dosR regulon) [21, 22]. Direct assessment of hypoxia *in vivo* typically involves the utilization of polarographic oxygen electrodes which can provide absolute measurements of tissue oxygenation at the sampling location. However, this procedure is technically demanding and suffers from a number of limitations including invasiveness, high susceptibility to sampling errors and the fact that only easily accessible locations can be interrogated [23]. [^{18}F]FMISO PET-CT scans define regions of hypoxia without the need for invasive probes, as previously shown in tumour biology [24] and cerebral ischaemia [25]. Since high tracer uptake, as quantified by standardized uptake value (SUV) or TBR, may represent high tracer delivery to a region of interest rather than tracer trapping under hypoxic conditions, we determined the influx rate of [^{18}F]FMISO into

the trapped tissue compartment (K_i) so as to more specifically identify tissue hypoxia. The maximum TB lesion K_i value (0.005 min^{-1}) is equal to the highest K_i value in an [^{18}F]FMISO study of head and neck cancer by Wang et al [26], which puts the degree of hypoxia in this study into context. Our data reveals that heterogeneity exists both within individual TB lesions and between lesions, consistent with the concept of multiple TB microenvironments existing within a single patient.

The finding of hypoxia within lung lesions directed our cellular experiments. MMP-1 gene expression and secretion were significantly increased in *M.tb*-infected human macrophages in hypoxia compared to normoxia and MMP-1 was functionally active. However, hypoxia had no effect on mycobacterial growth in our experiments. Diverse lines of investigation are implicating MMP-1 as a key protease in TB pathology. MMP-1 causes collagen destruction in *M.tb*-infected transgenic mice [6] and *M.tb* infection upregulates MMP-1 more potently than *M.bovis* BCG in human macrophages [15]. In pre-sensitized rabbits, MMP-1 has been shown to have a causal role in pulmonary cavitation [27]. Specifically, the development of cavities within areas of dense consolidation has been associated with MMP-1/TIMP imbalance and high intracavitary bacterial burden. In human TB granulomas, MMP-1 expression is up-regulated 606-fold compared to uninfected lung [28]. Similarly, MMP-1 was the most potently upregulated gene in macrophages from patients who developed TB compared with those with latent disease [29]. The effect of hypoxia was mimicked by chemically targeting the pathway with DMOG, which suggests that it may be possible to therapeutically manipulate the excess inflammatory response in TB using small molecules.

Hypoxia-dependent, monocyte driven up-regulation of MMP-1 gene expression in human respiratory epithelial cells required the transcription factor NF- κ B. NF- κ B and HIF-1 α interact to regulate innate immunity and inflammation [9, 10]. NF- κ B critically regulates MMP activity in TB infection of the central nervous system [30], but has not been investigated in the context of hypoxia-driven MMP expression in TB infection. NF- κ B is both directly affected by hypoxia and modulates HIF-1 α expression as well as being regulated by prolyl hydroxylases [31]. The precise nature of the interaction between HIF-1 α , prolyl hydroxylases and NF- κ B in TB is currently being investigated by our group.

M.tb caused significant accumulation of HIF-1 α in direct infection and via a networking effect even in the absence of hypoxia, with a synergistic increase in HIF-1 α expression in hypoxia or following treatment with DMOG. To our knowledge, this is the first time that hypoxia-independent HIF-1 α stabilization has been observed in any mycobacterial infection, although similar effects have been reported in other infections [32, 33]. Interestingly, recent gene expression profiling in peripheral whole blood demonstrated significant up-regulation of HIF-1 α gene expression in TB patients compared to controls [34]. Our findings are consistent with the demonstration of activation of HIF-1 α signalling pathways following infection in a zebrafish model of TB infection [35]. We showed expression of HIF-1 α within TB granulomas, localizing the activity to epithelioid macrophages and multi-nucleate giant cells, which we have previously shown are key in secretion of several MMPs [15]. We demonstrate that HIF-1 α regulates MMP-1 expression in TB. Since the chemical inhibitor LW6 can lack specificity we used targeted siRNA to confirm this finding. Consistent with our data in TB, hypoxia and HIF-1 α regulate MMP-driven tissue destruction in hypoxic fibroblasts within rheumatoid synovium [36].

In summary, we show for the first time that human TB lesions are severely hypoxic. Hypoxia increases MMP-1 gene expression and secretion during *M.tb* infection, and *M.tb* infection independently increases HIF-1 α activity even under conditions of normoxia. Taken together, our data suggests the *M.tb* drives a HIF-1 α -dependent proinflammatory tissue destructive cascade that may lead to cavitation and promote disease transmission, representing a potential future therapeutic target in the era of increasing drug resistant TB.

FOOTNOTES

Acknowledgements

The authors would like to acknowledge Dr Rob Smith and Robert Bielik, Wolfson Brain Imaging Centre, University of Cambridge for their support in coordinating synthesis and transportation of [¹⁸F]FMISO.

Funding

Supported by Medical Research Council (UK) Clinical Research Training Fellowships (MB, JG), Wellcome Trust Clinical Research Training Fellowship (RM), Fundacao Ciencia Tecnologia, Portugal (SB), Imperial College Healthcare Charity, UK , The Mason Medical Research Foundation UK grant, NIHR Cambridge Biomedical Research Centre (RM), and The Imperial College Biomedical Research Centre UK (PE, JSF).

Declaration of interests

None

Author contributions

M.B., T.D.F., Y.T.H., F.A., K.N, A.A., P.T.E., and J.S.F conceived and designed the clinical study, and M.B., N.H.P., R.M., Y.T.H., and T.D.F collected and analyzed the clinical data. M.B. recruited the clinical cohort. M.B., S.B., L.T., J.G., M.D. and R.M. were involved in the cellular studies. F.A.M. performed the histological analysis. All authors contributed to the writing of the manuscript and approved the final submitted version.

REFERENCES

1. WHO, *Global Tuberculosis Report 2012*. 2012.
2. Helke, K.L., J.L. Mankowski, and Y.C. Manabe, *Animal models of cavitation in pulmonary tuberculosis*. *Tuberculosis*, 2006. **86**(5): p. 337-348.
3. Via, L.E., et al., *Tuberculous Granulomas Are Hypoxic in Guinea Pigs, Rabbits, and Nonhuman Primates*. *Infection and Immunity*, 2008. **76**(6): p. 2333-2340.
4. Harper, J., et al., *Mouse Model of Necrotic Tuberculosis Granulomas Develops Hypoxic Lesions*. *Journal of Infectious Diseases*, 2012. **205**(4): p. 595-602.
5. Volkman, H.E., et al., *Tuberculous Granuloma Induction via Interaction of a Bacterial Secreted Protein with Host Epithelium*. *Science*, 2010. **327**(5964): p. 466-469.
6. Elkington, P., et al., *MMP-1 drives immunopathology in human tuberculosis and transgenic mice*. *J Clin Invest*, 2011. **121**(5): p. 1827-33.
7. Walker, N.F., et al., *Doxycycline and HIV Infection Suppress Tuberculosis-induced Matrix Metalloproteinases*. *American Journal of Respiratory and Critical Care Medicine*, 2012. **185**(9): p. 989-997.
8. Nizet, V. and R.S. Johnson, *Interdependence of hypoxic and innate immune responses*. *Nat Rev Immunol*, 2009. **9**(9): p. 609-617.
9. Rius, J., et al., *NF- κ B links innate immunity to the hypoxic response through transcriptional regulation of HIF-1 α* . *Nature*, 2008. **453**(7196): p. 807-811.
10. Eltzschig, H.K. and P. Carmeliet, *Hypoxia and Inflammation*. *New England Journal of Medicine*, 2011. **364**(7): p. 656-665.
11. Semenza, G.L., *HIF-1: mediator of physiological and pathophysiological responses to hypoxia*. *Journal of Applied Physiology*, 2000. **88**(4): p. 1474-1480.
12. Schofield, C.J. and P.J. Ratcliffe, *Oxygen sensing by HIF hydroxylases*. *Nat Rev Mol Cell Biol*, 2004. **5**(5): p. 343-354.
13. Huang, L.E., et al., *Regulation of hypoxia-inducible factor 1 α is mediated by an O₂-dependent degradation domain via the ubiquitin-proteasome pathway*. *Proceedings of the National Academy of Sciences*, 1998. **95**(14): p. 7987-7992.
14. Semenza, G.L., *HIF-1, O₂, and the 3 PHDs: How Animal Cells Signal Hypoxia to the Nucleus*. *Cell*, 2001. **107**(1): p. 1-3.
15. Elkington, P.T.G., et al., *Mycobacterium tuberculosis, but Not Vaccine BCG, Specifically Upregulates Matrix Metalloproteinase-1*. *American Journal of Respiratory and Critical Care Medicine*, 2005. **172**(12): p. 1596-1604.
16. Elkington, P.T.G., et al., *Mycobacterium tuberculosis Up-Regulates Matrix Metalloproteinase-1 Secretion from Human Airway Epithelial Cells via a p38 MAPK Switch*. *The Journal of Immunology*, 2005. **175**(8): p. 5333-5340.
17. Kizaka-Kondoh, S. and H. Konse-Nagasawa, *Significance of nitroimidazole compounds and hypoxia-inducible factor-1 for imaging tumor hypoxia*. *Cancer Science*, 2009. **100**(8): p. 1366-1373.
18. Lawrentschuk, N., et al., *Assessing regional hypoxia in human renal tumours using 18F-fluoromisonidazole positron emission tomography*. *BJU International*, 2005. **96**(4): p. 540-546.
19. Gagel, B., et al., *pO₂ Polarography Versus Positron Emission Tomography ([18F] Fluoromisonidazole, [18F]-2-Fluoro-2'-Deoxyglucose)*. *Strahlentherapie und Onkologie*, 2004. **180**(10): p. 616-622.
20. Prekeges, J.L., et al., *Reduction of fluoromisonidazole, a new imaging agent for hypoxia*. *Biochem Pharmacol*, 1991. **42**(12): p. 2387-95.
21. Gideon, H.P., et al., *Hypoxia Induces an Immunodominant Target of Tuberculosis Specific T Cells Absent from Common BCG Vaccines*. *PLoS Pathog*, 2010. **6**(12): p. e1001237.

22. Honaker, R.W., et al., *Unique Roles of DosT and DosS in DosR Regulon Induction and Mycobacterium tuberculosis Dormancy*. Infection and Immunity, 2009. **77**(8): p. 3258-3263.
23. Mortensen, L.S., et al., *Identifying hypoxia in human tumors: A correlation study between 18F-FMISO PET and the Eppendorf oxygen-sensitive electrode*. Acta Oncologica, 2010. **49**(7): p. 934-940.
24. Carlin, S. and J.L. Humm, *PET of Hypoxia: Current and Future Perspectives*. Journal of Nuclear Medicine, 2012. **53**(8): p. 1171-1174.
25. Takasawa, M., et al., *Single-subject statistical mapping of acute brain hypoxia in the rat following middle cerebral artery occlusion: A microPET study*. Experimental Neurology, 2011. **229**(2): p. 251-258.
26. Wang, W., et al., *Pharmacokinetic Analysis of Hypoxia 18F-Fluoromisonidazole Dynamic PET in Head and Neck Cancer*. Journal of Nuclear Medicine, 2010. **51**(1): p. 37-45.
27. Kubler, A., et al., *Mycobacterium tuberculosis dysregulates MMP/TIMP balance to drive rapid cavitation and unrestrained bacterial proliferation*. J Pathol, 2015. **235**(3): p. 431-44.
28. Kim, M.-J., et al., *Casation of human tuberculosis granulomas correlates with elevated host lipid metabolism*. EMBO Molecular Medicine, 2010. **2**(7): p. 258-274.
29. Caws, M., et al., *The Influence of Host and Bacterial Genotype on the Development of Disseminated Disease with *Mycobacterium tuberculosis**. PLoS Pathog, 2008. **4**(3): p. e1000034.
30. Green, J.A., et al., *Mycobacterium tuberculosis-infected human monocytes down-regulate microglial MMP-2 secretion in CNS tuberculosis via TNFalpha, NFkappaB, p38 and caspase 8 dependent pathways*. J Neuroinflammation, 2011. **8**: p. 46.
31. Fujita, N., et al., *Prolyl hydroxylase 3 (PHD3) modulates catabolic effects of tumor necrosis factor-alpha (TNF-alpha) on cells of the nucleus pulposus through co-activation of nuclear factor kappaB (NF-kappaB)/p65 signaling*. J Biol Chem, 2012. **287**(47): p. 39942-53.
32. Haeberle, H.A., et al., *Oxygen-Independent Stabilization of Hypoxia Inducible Factor (HIF)-1 during RSV Infection*. PLoS ONE, 2008. **3**(10): p. e3352.
33. Peyssonnaud, C., et al., *HIF-1alpha expression regulates the bactericidal capacity of phagocytes*. The Journal of Clinical Investigation, 2005. **115**(7): p. 1806-1815.
34. Maertzdorf, J., et al., *Common patterns and disease-related signatures in tuberculosis and sarcoidosis*. Proceedings of the National Academy of Sciences, 2012. **109**(20): p. 7853-7858.
35. Elks, P.M., et al., *Hypoxia Inducible Factor Signaling Modulates Susceptibility to Mycobacterial Infection via a Nitric Oxide Dependent Mechanism*. PLoS Pathog, 2013. **9**(12): p. e1003789.
36. Lee, Y.-A., et al., *Hypoxia differentially affects IL-1beta-stimulated MMP-1 and MMP-13 expression of fibroblast-like synoviocytes in an HIF-1alpha-dependent manner*. Rheumatology, 2012. **51**(3): p. 443-450.

FIGURE LEGENDS

Figure 1. [^{18}F]FMISO PET-CT demonstrates increased tracer uptake within TB lesions

(A) [^{18}F]FMISO PET-CT images. Transverse, coronal and sagittal slices through the [^{18}F]FMISO target-to-background (TBR) and CT images of patient 2. Top row, CT images show consolidation and a pulmonary cavity in the right upper lobe with a smaller, non-cavitating lesion in the left lung. Middle row, [^{18}F]FMISO TBR map demonstrates intense uptake of tracer in the right upper lobe lesion and the liver, the site of metabolism of [^{18}F]FMISO. Bottom row, co-registered CT and TBR images. (B) Target-to-background (TBR) values greater than unity were found for at least one lesion in all patients (each individual bar represents one region of interest, ROI).

Figure 2. Severe hypoxia is present within human pulmonary TB lesions

(A) Patlak K_i images from dynamic PET-CT scanning for Patient 2 demonstrate intense retention of [^{18}F]FMISO in the right upper lobe of the lung (middle row). Co-registered PET-CT images (bottom row) confirm localization of hypoxia to the region of the right upper lobe cavity. (B) Regional K_i values demonstrate heterogenous trapping of [^{18}F]FMISO within and between patients. The hypoxia threshold (0.00037 min^{-1}) was determined from the mean + 3 standard deviations of the K_i values in the normoxic lateral muscle background regions across the patient group. (C) Time-activity measurements of five ROIs from patient 3 demonstrate high tissue levels compared to peripheral blood values.

Figure 3. Hypoxia increases *M.tb*-driven MMP-1 expression and secretion by human monocyte-derived macrophages (MDMs).

(A) Hypoxia (1% pO₂) increases MMP-1 gene expression in primary human MDMs infected with *M.tb* at 24 hours. (B) Hypoxia increases intracellular MMP-1 accumulation on confocal microscopy at 72hrs in MDMs infected with *M.tb* (MOI=1) compared to normoxia or control uninfected cells. (C) Mtb infection increases MMP-1 secretion by infected MDMs greater than LPS (100ng/ml) in both normoxia and hypoxia analyzed 72h after infection. (D) MMP-1 activity is increased in *M.tb*-infected but not control human macrophages analyzed by casein zymography, and hypoxia further increases caseinolytic activity. (E) Stabilization of HIF-1 α by DMOG (range 0.05-0.5mM) significantly increases MMP-1 secretion analyzed by ELISA and proteolytic activity measured by zymography in a dose-dependent manner. N = 21% O₂; 5% CO₂, H = 1% O₂; 5% CO₂. **** p < 0.0001, *** p < 0.001, ** p < 0.01, * p < 0.05.

Figure 4. Hypoxia upregulates MMP-1 in human respiratory epithelial cells.

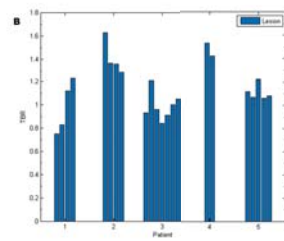
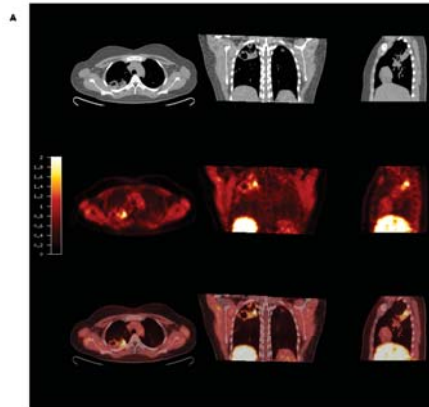
(A) Hypoxia increases MMP-1 secretion from NHBE cells stimulated with control medium or CoMTb incubated in 21%, 5% or 1% oxygen. (B) DMOG (range 0.1-0.25mM) drives dose-dependent MMP-1 secretion from CoMTb-stimulated NHBE cells. (C) *In silico* analysis of the MMP-1 promoter reveals putative hypoxic response element (HRE) binding sites as well as consensus NF- κ B and AP-1 binding sites. (D) Relative luminescence following transfection of A549 respiratory epithelial cells with either WT-MMP-1 promoter or a series of MMP-1 promoter deletion constructs in normoxia (solid bars) or hypoxia (shaded bars). The effect of hypoxia in increasing promoter activity is absent in constructs -1551, -1194 and -517. (E) IKK β inhibition in hypoxia with SC-514 in CoMTb stimulated cells resulted in a dose-dependent decrease in MMP-1 secretion. (F) Site-directed mutagenesis of the NF- κ B binding site at -2878 to -2886bp decreases MMP-1 promoter activity in response to CoMTb in normoxia (solid bars) or hypoxia (shaded bars). ** p < 0.01, * p < 0.05.

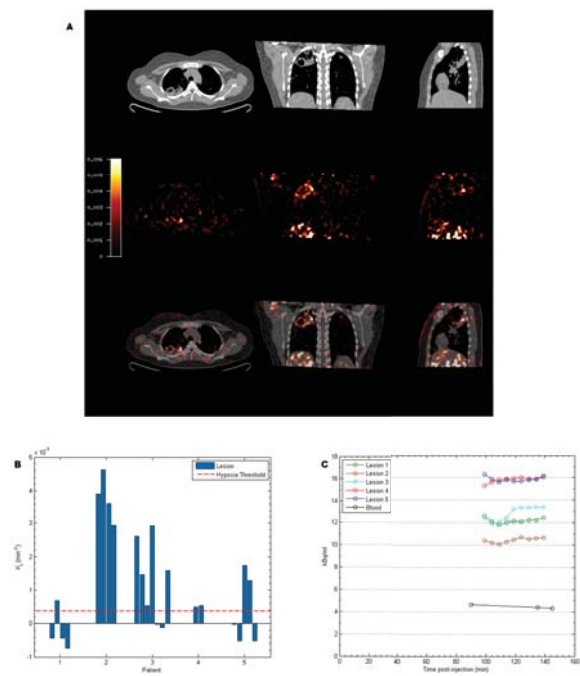
Figure 5. *M.tb* infection drives HIF-1 α accumulation in normoxia

(A) In A549 cells, CoMTb stimulation and DMOG (0.25mM) results in early HIF-1 α stabilization. Pre-incubating A549 cells with DMOG (0.25mM) and subsequent stimulation with CoMTb markedly increases HIF-1 α accumulation, peaking at 6 hrs. (B) *M.tb* infection increases HIF-1 α accumulation and stabilization in normoxia in primary human MDMs, peaking at 24hrs. (C) Combined infection with *M.tb* and exposure to hypoxia causes greater HIF-1 α accumulation than either stimulus alone, peaking at 4hrs and persisting until 24hr. (D) Inhibition of HIF-1 α by LW6 (range 50-100 μ M) results in decreased MMP-1 secretion in *M.tb*-infected MDMs in hypoxia (hatched bars). ** $p < 0.01$.

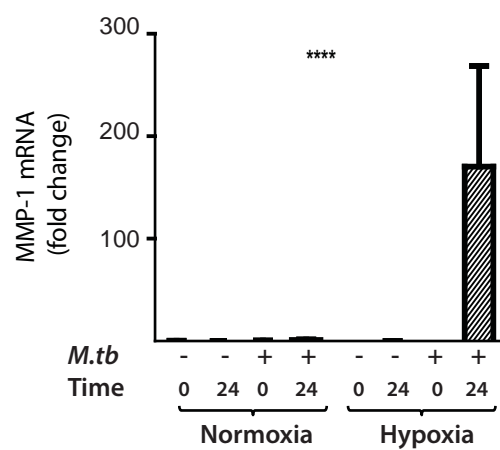
Figure 6. HIF-1 α is necessary for MMP-1 gene expression and secretion during *M.tb* infection.

(A) HIF-1 α western blot at 24hrs demonstrates suppression of HIF-1 α protein by HIF-1 α siRNA in MDMs in both normoxia and hypoxia, with no knockdown observed with non-targeting (NT) siRNA. (B) HIF-1 α siRNA decreases MMP-1 gene expression at 24hrs in *M.tb* infected MDMs incubated in hypoxia. (C) HIF-1 α siRNA causes a significant decrease in MMP-1 secretion at 48hrs under conditions of normoxia (solid bars) and hypoxia (hatched bars). No significant change in MMP-1 gene expression or secretion is seen with non-targeting siRNA. (D) Lung biopsies from patients with pulmonary TB (i, ii) are immunoreactive for HIF-1 α compared with uninfected control biopsies (iii). HIF-1 α staining is pronounced within macrophages and multinucleated giant cells (arrow, ii). Scale bars, 100 μ m. **** $p < 0.0001$, * $p < 0.05$.

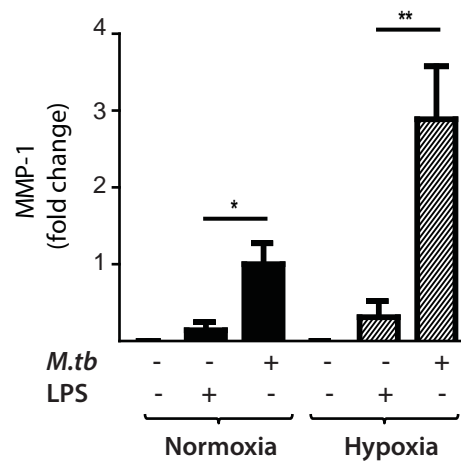




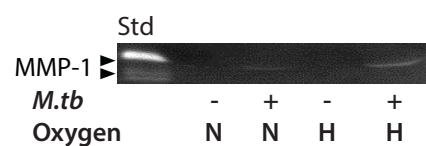
A



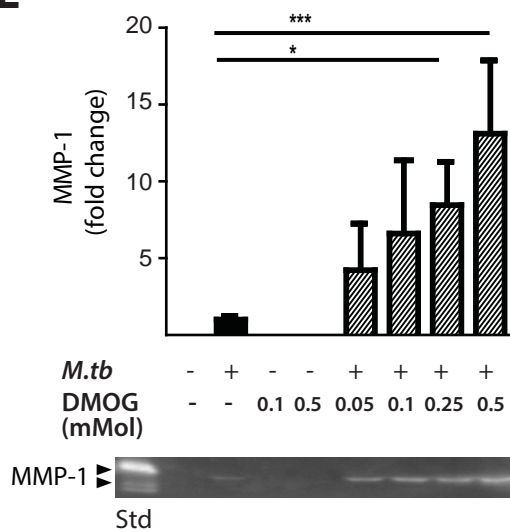
C

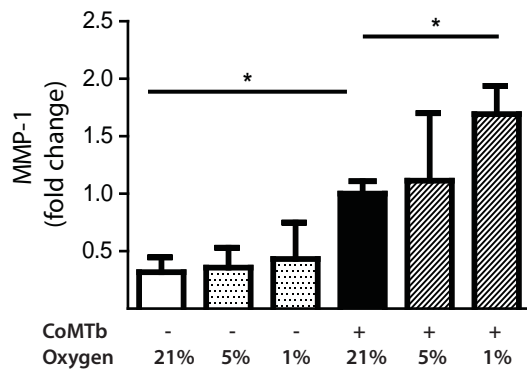
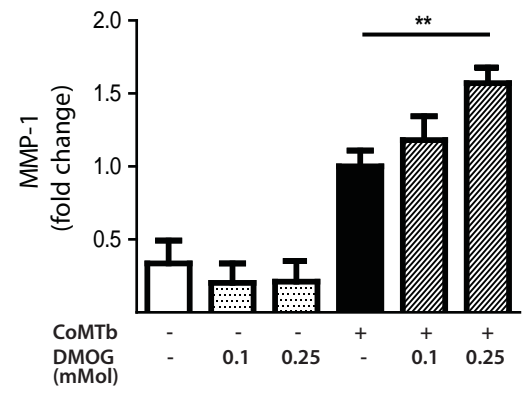
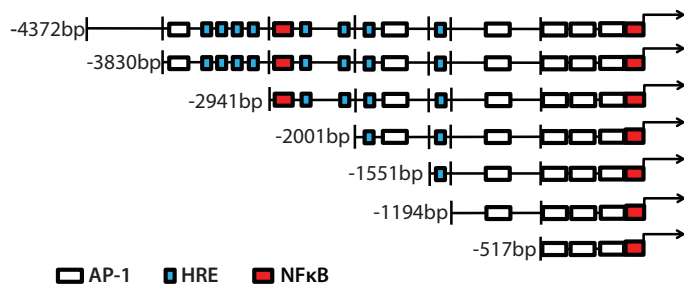
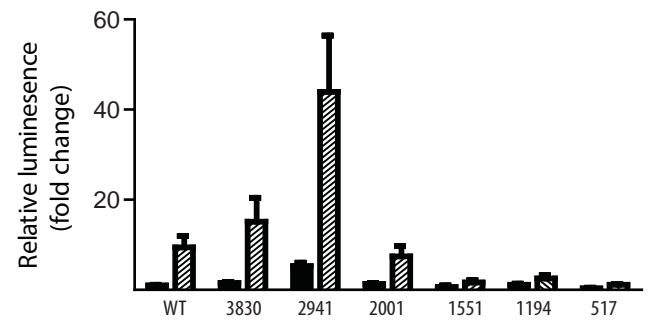
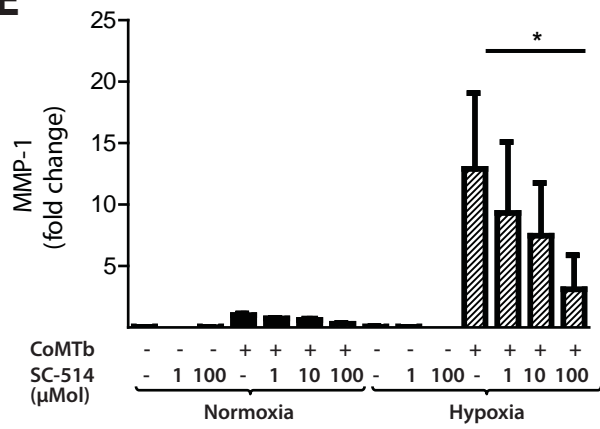
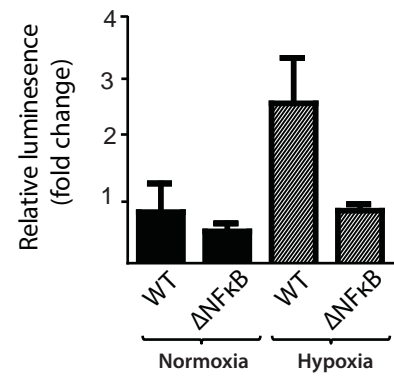


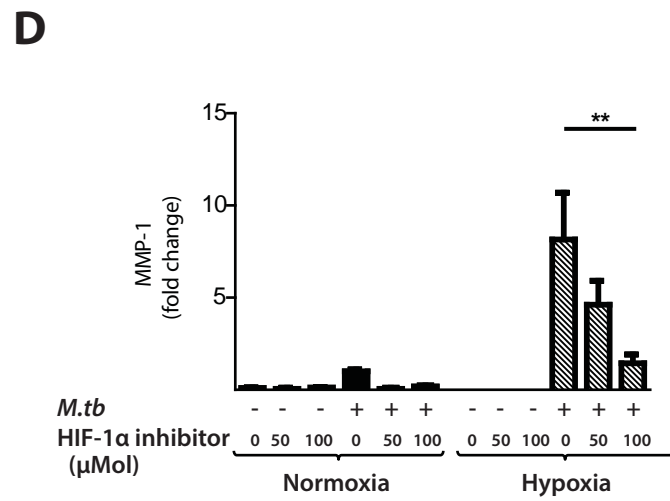
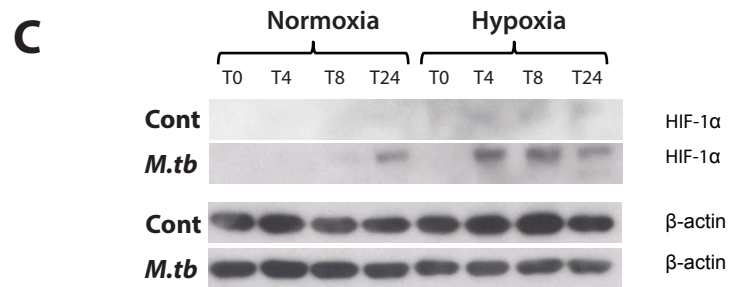
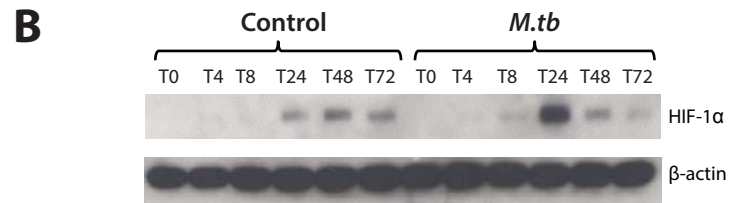
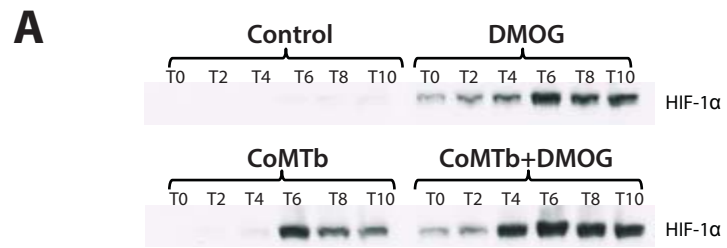
D

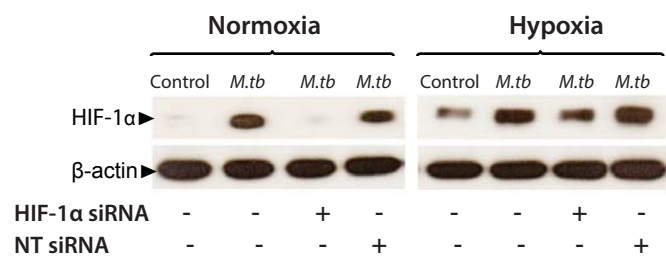
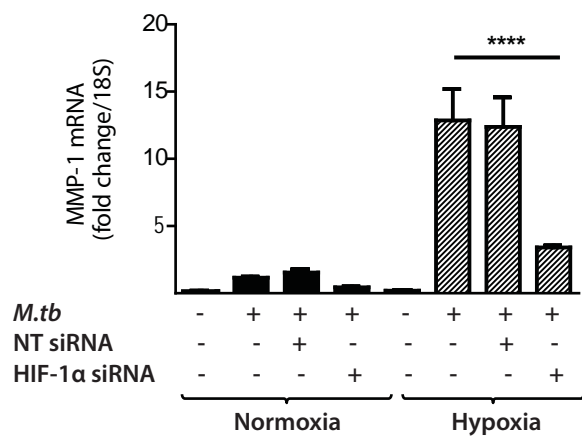
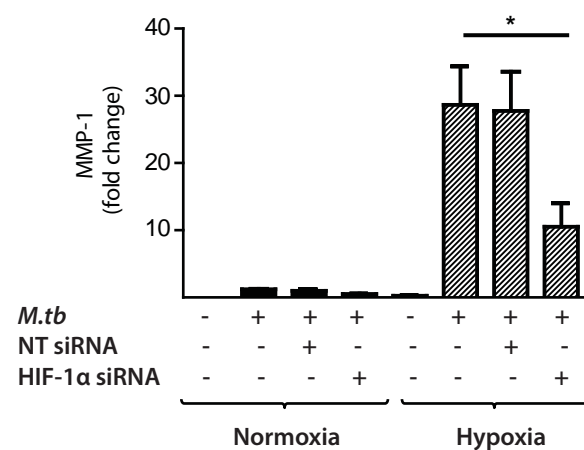


E

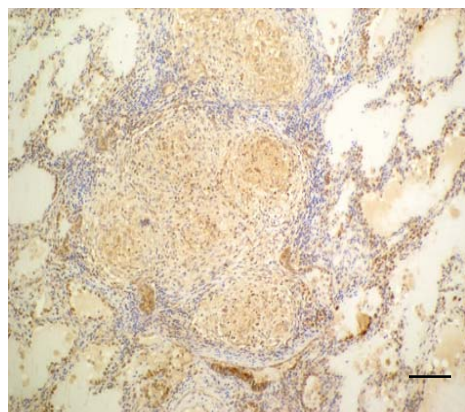


A**B****C****D****E****F**

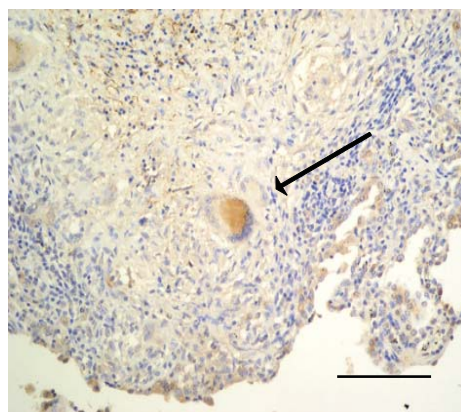


A**B****C****D**

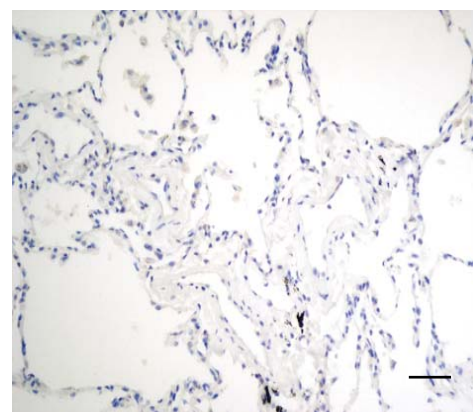
(i)



(ii)



(iii)



Hypoxia and HIF-1 α -dependent MMP-1 secretion in human pulmonary
tuberculosis

Moerida Belton, Sara Brilha, Roido Manavaki , Francesco Mauri, Kuldip Nijran,
Young T Hong, Neva Patel, Marcin Dembek, Liku Tezera, Justin Green,
Rachel Moores, Franklin Aigbirhio, Adil Al-Nahhas, Tim D Fryer, Paul T
Elkington, Jon S Friedland

Online data supplement

Methods

¹⁸F-FMISO PET-CT scans

PET-CT scans were performed on a Siemens mCT (Siemens Medical, Erlangen, Germany) at the Department of Nuclear Medicine Charing Cross Hospital, Imperial College NHS Trust, London. [¹⁸F]FMISO was synthesized in the Wolfson Brain Imaging Centre, Cambridge University. Patients received 406 ± 6 MBq [¹⁸F]FMISO intravenously followed by a 90 minute uptake period to promote contrast between normoxic and hypoxic tissue on tissue-to-background (TBR) images, and also to allow the free [¹⁸F]FMISO concentration in tissue to reach equilibrium with that in blood, a pre-requisite for Patlak plot determination of influx rate (K_i) [1]. Immediately following a low dose CT scan for attenuation correction, patients underwent a 45 minute single bed position PET scan acquired in list mode. As Patlak analysis requires knowledge of the input function to the tissue, three venous blood samples (90, 135 and 145 minutes post-injection) were taken in order to scale to a population-based [¹⁸F]FMISO arterial plasma function. The latter was produced from 6 controls scanned at The Wolfson Brain Imaging Centre, University of Cambridge as part of a study on stroke (PI: Prof J-C Baron), which included late venous sampling as part of the study protocol.

[¹⁸F]FMISO PET-CT data analysis

List mode PET data were reconstructed into 9x5min frames using OSEM [2] (8 subsets, 4 iterations, 5mm FWHM 3D Gaussian post-smoothing filter) into a 168x168x74 array with voxel dimensions 4.07 x 4.07 x 3.00mm. Corrections were applied for randoms, dead time, normalization, scatter, attenuation, sensitivity and radioactive decay. To reduce the impact

of patient motion during PET acquisition, the last 8 frames of the dynamic PET image series were non-rigidly registered to the first frame using symmetric normalization (SyN) with mutual information as the similarity metric [3]. All PET frames were then registered to CT using affine transformation. The last three of the registered frames (120-135mins post injection) were converted to a TBR image through normalization with the radioactivity concentration in a bilateral lateral muscle region assumed to represent normoxic tissue. All 9 frames were used to produce a K_i map using Patlak plot analysis. Regions of interest (ROI) were defined on the TBR images and ROI values were determined by placing the ROIs on the TBR and K_i maps.

***M.tb* culture**

M.tuberculosis H375v was cultured in Middlebrook 7H9 medium supplemented with 10% OADC enrichment medium (BD Biosciences, Oxford, UK), 0.2% glycerol and 0.02% Tween 80. Cultured cells were infected with *M.tb* at mid-logarithmic growth at an optical density of 0.6 (Biowave cell density meter, WPA, Cambridge, UK). To count intracellular bacilli, infected MDMs were lysed with 0.1% Triton-X. Aliquots of cell lysates were serially diluted 10-fold in 7H9 liquid and 4 dilutions of each sample were plated on 7H11 agar and incubated for 14 days before determining the number of CFU.

Monocyte Purification and Maturation

Monocytes were isolated from single donor leucocyte cones (National Blood Transfusion Service, London, UK) by density gradient centrifugation (Amersham Biosciences) and re-

suspended in RPMI. Monocytes were purified by adhesion for 1 hour followed by washing 6 times in HBSS to remove non-adherent cells. Monocytes were matured for 4 days in 100ng/ml M-CSF and then rested for 1 day in RPMI containing no M-CSF. The resultant monocyte-derived macrophages (MDMs) were infected with *M.tuberculosis* H37RV at an MOI of 1. MMP gene expression was analyzed at 24 hours and MMP secretion measured at 3 days after infection. Conditioned media from *M.tb* infected monocytes (CoMTb) was produced by infecting monocytes at a multiplicity of infection (MOI) of 1. After 24 hours, cell culture medium was harvested, centrifuged at 13,000rpm for 5 minutes and filtered to remove infectious material using a 0.2µm Anopore filter (Whatman, UK) [4].

Epithelial cell culture

Normal human bronchial epithelial cells (NHBE) (Lonza, Basel, Switzerland) and the human type II alveolar A549 cell line were acquired as cryopreserved cells and regenerated according to the manufacturers' instructions. A549 cells were maintained in RPMI 1640 with 10% FCS, 2mM glutamine, and 10mg/ml ampicillin. Experiments were performed on cells between passage 8-16 and unless otherwise stated, cell culture supernatants were harvested at 72 hours and MMPs analysed by ELISA or Luminex array. Cell viability was assessed by trypan blue exclusion. Chemical inhibition experiments were performed using dimethyloxalylglycine (DMOG conc. range 0.05-0.5mM) (Inochem, Carnforth, UK), helenalin SC-514 (conc. range 1-100µM) and 3-(2-(4-Adamantan-1-yl-phenoxy)-acetylamino)-4-hydroxybenzoic acid methyl ester, LW6 (conc. range 50-100µM) (all MerckMillipore, Darmstadt, Germany). All inhibitors were dissolved in DMSO according to manufacturers instructions.

Hypoxia workstation

A custom designed hypoxia workstation was commissioned for the biological safety level 3 facility (Coy Laboratories, USA). The workstation comprised a sealed environment with an inbuilt humidified incubator accessed by air-tight gloves. Materials and reagents were passed in and out of the workstation via a sealed airlock, such that the atmosphere remained constant at all times. Temperature and CO₂ were maintained at 37°C and 5% respectively and O₂ levels (by N₂ displacement) adjusted according to the experimental requirements. All parameters were monitored by digital sensors throughout and adjustments made automatically. In experiments comparing multiple oxygen levels, a hypoxic incubator was also used for 5% O₂ (Galaxy 14S, New Brunswick, UK)

Casein Zymography

To analyze MMP-1 activity, samples were electrophoresed on 0.05% casein gels (Invitrogen) and incubated in collagenase buffer at 37°C for 48h. All gels were run with a 5ng recombinant MMP-1 (Calbiochem, Merck Biosciences, UK) to standardise between gels. Caseinolytic activity was revealed by Coomassie blue staining (Pharmacia) for one hour followed by destain in methanol: acetic acid: water [5].

Real-time PCR

Macrophages were lysed using Tri-Reagent (Sigma-Aldrich, Dorset, UK), and total RNA was extracted using PureLink RNA® Mini Kit (Invitrogen, Paisley, UK). 1µg RNA was reverse transcribed using QuantiTect Reverse Transcriptase Kit (Qiagen, Manchester, UK). qPCR reactions were performed in an ABI Prism 7700 (Applied Biosystems, Paisley, UK). MMP-1

cycle thresholds were quantified by comparison to an MMP-1 standard curve generated using known MMP-1 concentrations generated from a plasmid standard and then standardised to 18S rRNA. HIF-1 α mRNA samples were analysed using the comparative threshold method. The Ct values of both calibrator and samples were normalized to 18S rRNA.

Measurement of MMP and TIMP concentrations

Total MMP and TIMP secretion in cell culture supernatants was measured by ELISA (R&D Systems, Abdingdon, UK) or on the Luminex 200 platform using MMP Luminex multiplex array (R&D Systems, Abingdon, UK) according to the manufacturer's instructions. The minimum level of detection for MMP-1 was 10 pg/ml.

HIF-1 α Western analysis

Cells were washed 3 times in sterile PBS and then lysed in SDS sample buffer (62.5mM Tris, 2% SDS, 10% glycerol, 50mM DDT, 0.01% bromophenol blue). For macrophages directly infected with *M.tb* H37RV, samples were sterile filtered through a 0.2 μ m Anopore filter (Whatman, UK). After heat-denaturation, samples were separated by electrical gradient on a NuPAGE Bis-Tris 4-12% gel (Invitrogen, Paisley, UK), electro-transferred to a nitrocellulose membrane (Amersham, UK) and blocked with 5% milk protein/0.1% Tween-20. The membrane was probed with anti-HIF1 α Ab (1:1,000 dilution) (BD Biosciences, UK) overnight, washed, and incubated with goat anti-mouse IgG horseradish peroxidase (HRP)-conjugate secondary Ab (1:1,000 dilution, Jackson ImmunoResearch). Loading control was performed

using the rabbit-anti β -actin Ab (1:5,000 dilution) and goat anti-mouse IgG horseradish peroxidase (HRP)-conjugate secondary Ab (1:5,000 dilution, Jackson ImmunoResearch). Luminescence was detected with the ECL system (Amersham, UK) according to manufacturer's protocol.

Confocal microscopy

Primary human monocytes were matured to macrophages in 4-well Permanox plastic chamber slides (Thermo Fisher Scientific Inc. UK). Cells were fixed for 3 days following infection with 4% paraformaldehyde in PBS for 30 minutes. Cells were permeabilized with 0.5% saponin and blocked with 1% BSA for 1 hr. Cells were incubated with anti-MMP-1 primary Ab (1:200, Abcam, UK) overnight, washed and incubated with goat anti-mouse secondary Ab (1:100, Abcam, UK) and labelled with FITC for 2 hrs. Nuclei were visualized using DAPI. The images were scanned under an x60 oil immersion objective and to avoid bleed-through effects, each dye was scanned independently by a Leica TCS SP5 equipped with an argon-krypton mixed gas laser. Image analysis was with Leica confocal software (Leica Microsystems, Germany) and Image J v1.48a.

Promoter-reporter assay

A549 cells were transfected with either wild-type, truncation or deletion constructs of the MMP-1 promoter DNA inserted into the firefly luciferase expression plasmid pGL2-basic (gift from Dr. I. Clarke, University of East Anglia, U.K.) and control reporter plasmid, pRL-TK, constitutively expressing *Renilla* luciferase activity, with FuGene 6 (Roche) [6]. Cells were

stimulated with CoMTb in the presence or absence of hypoxia then lysed after 24 h. Luciferase activity was measured using the Dual-Luciferase Reporter Assay System (Promega, Southampton, UK) analyzed with the Bio-Orbit 1253 luminometer (Labtech International). *Renilla* luciferase activity was used to normalize firefly activity to control for transfection efficiency.

siRNA

Monocytes were isolated and differentiated into MDMs. MDMs were transfected using DharmaFECT 3 transfection reagent with either non-targeting control siRNA or HIF-1 α siRNA smartpool (Dharmacon, FisherScientific, Loughborough, UK), according to the supplier's instructions. Transfection medium was replaced with RPMI at 8hrs and cells allowed to rest for 16hrs, at which time the MDMs were infected with *M.tb* H37Rv (MOI= 1). Cell culture supernatant and cell lysates were harvested for HIF-1 α and MMP-1 mRNA and protein secretion analyses. To assess transfection efficiency, MDMs were also transfected with 25nM FAM conjugated non-targeting control siRNA, detached from the plates with cell dissociation buffer (Gibco, Invitrogen) and analysed by flow cytometry (FACSCalibur, BD Biosciences).

Immunohistochemistry

HIF-1 α immunohistochemistry was performed on formalin-fixed, paraffin-embedded lung biopsies from six patients with culture-proved *M.tb* infection and six non-infected control samples. Immunohistochemistry staining was performed using Bond III fully automated staining system with the Bond Polymer Refine Detection system and associated reagents

(Leica Microsystems, Newcastle-Upon-Tyne, UK). Antigen retrieval was carried out using Epitope retrieval pH 6 (ER1) at 100°C for 30mins. The antibody HIF1- α (Abcam AB1) was applied for 30mins at a dilution of 1/500. The detection system uses DAB as chromogen and section were counterstained with haematoxylin.

Statistics

Statistical analysis was performed using GraphPad PRISM 6. Data was analyzed with one-way ANOVA and Tukey's post-test performed to account for multiple comparison of variables. A *P* value of 0.05 was considered significant. For all experiments, bars represent mean values of 3 samples \pm SD. All graphs are representative of at least duplicate experiments.

References

1. Patlak, C.S., R.G. Blasberg, and J.D. Fenstermacher, *Graphical Evaluation of Blood-to-Brain Transfer Constants from Multiple-Time Uptake Data*. J Cereb Blood Flow Metab, 1983. **3**(1): p. 1-7.
2. Hudson, H.M. and R.S. Larkin, *Accelerated image reconstruction using ordered subsets of projection data*. Medical Imaging, IEEE Transactions on, 1994. **13**(4): p. 601-609.
3. Avants, B.B., et al., *Symmetric diffeomorphic image registration with cross-correlation: Evaluating automated labeling of elderly and neurodegenerative brain*. Medical Image Analysis, 2008. **12**(1): p. 26-41.
4. Elkington, P., *Filter sterilization of highly infectious samples to prevent false negative analysis of matrix metalloproteinase activity*. J Immunol Methods, 2006. **Feb 20**: p. 309(1-2).
5. Troeberg, L. and H. Nagase, *Zymography of Metalloproteinases*, in *Current Protocols in Protein Science*. 2001, John Wiley & Sons, Inc.
6. O'Kane, C.M., et al., *STAT3, p38 MAPK, and NF-kappaB drive unopposed monocyte-dependent fibroblast MMP-1 secretion in tuberculosis*. Am J Respir Cell Mol Biol, 2010. **43**(4): p. 465-74.

	Patient 1 1P	Patient 2	Patient 3	Patient 4	Patient 5
Sex (M/F)	M	F	F	F	F
Age (years)	49	22	31	37	62
Country of origin	Romania	Mongolia	Nepal	Philippines	Morocco
Height (cm)	178	160	153	157	156
Weight (kg)	64	53.2	44.9	45.3	48
Duration of symptoms	6 months	3 months	1 month	1 month	1 month
Symptoms					
Cough	+	+	+	+	+
Weight loss	+	-	+	+	-
Fever	+	+	+	+	+
Haemoptysis	+	-	-	-	-
GI symptoms	-	-	+	-	-
Lethargy	-	-	-	-	+
Smoking status	Current 30 pack years	Never	Never	Never	Never
CXR					
Consolidation	+	+	+	+	+
Cavitation	+	+	-	+	+
Fibrosis	-	-	+	-	-
Sputum smear	AFB +++	AFB +++	AFB +	AFB +	AFB +++
Days to <i>M.tb</i> culture positivity	3 days	7 days	26 days	7 days	5 days
Antibiotic sensitivity	Fully sensitive	Resistant isoniazid + streptomycin	Fully sensitive	Resistant rifampicin, isoniazid + prothionomide	Fully sensitive

Supplementary Table 1. Patient demographics, chest radiograph and microbiology results

	Patient 1t 1	Patient 2	Patient 3	Patient 4	Patient 5
Haematology					
Hb (g/dl)	10.8	10.2	10.1	12.7	10.4
WCC (x10 ⁹ g/l)	7.5	7.7	10.4	16.4	10.7
Neutrophil (x10 ⁹ g/l)	6.0	4.4	7.3	12.8	8.7
Biochemistry					
Na (mmol/l)	129	141	134	132	132
K+ (mmol/l)	4.0	4.1	4.8	4.0	4.0
Urea (mmol/l)	3.5	3.5	2.4	3.1	8.1
Cr (μmol/l)	52	53	55	65	97
CRP (mg/l)	189	10.6	150	69	312
Liver function					
Bilirubin (μmol/l)	10	n/a	6	11	12
ALT (IU/l)	39	n/a	13	29	<6
ALP (IU/l)	135	n/a	95	114	113
Total protein (g/l)	62	n/a	70	72	75
Albumin (g/l)	39	n/a	27	24	49
HIV status	Negative	Negative	Negative	Negative	Negative
Vitamin D (nmol/l)	26.0	28.6	24.3	25.9	14.9

Supplementary Table 2. Blood analysis at time of presentation

n/a, not available

Supplementary Table 3. Appearance on CT and binary hypoxic scale for each lesion examined.

Patient number	Lesion number	CT appearance	Hypoxic*
1	1	Consolidation	-
	2	Consolidation	+
	3	Consolidation	-
	4	Consolidation	-
2	1	Consolidation	+
	2	Consolidation	+
	3	Cavity wall	+
	4	Consolidation	+
3	1	Consolidation	+
	2	Consolidation	+
	3	Consolidation	+
	4	Consolidation	+
	5	Consolidation	-
	6	Consolidation	-
	7	Consolidation	+
4	1	Cavity wall	+
	2	Cavity wall	+
5	1	Cavity wall	-
	2	Cavity wall	-
	3	Consolidation	+
	4	Consolidation	+
	5	Consolidation	-

*The binary hypoxic scale denotes whether the lesion ROI Ki value is above a hypoxia threshold (0.00037 min^{-1}) determined from the mean + 3SD of the Ki values within the lateral muscle background ROIs, assumed to represent normoxic tissue.

Figure Legends Supplementary figures

Figure S1. Hypoxia does not cause cytotoxicity in NHBE cells

NHBE cells were stimulated with CoMTb and incubated in normoxia or hypoxia (1% or 5% pO₂; 5% CO₂). Supernatant were harvested at 72 hrs. Hypoxia did not cause an increase in LDH release in either control or CoMTb stimulated cells.

Figure S2. DMOG up-regulates MMP-9 secretion in NHBE cells stimulated with CoMTb.

NHBE cells were pre-incubated with DMOG (0.25mM) for 2 hours before stimulation with CoMTb. Supernatants were harvested at 72 hours. (A) Gelatin zymography shows DMOG increases MMP-9 gelatinolytic activity compared to control cells. A marked increase in MMP-9 proteolytic activity is seen in CoMTb stimulated cells. (B) DMOG and CoMTb stimulation increases MMP-9 secretion compared to cells treated with DMOG or CoMTb alone. *p<0.05

Figure S3. Hypoxia and DMOG up-regulates MMP-1 secretion in A549 cells stimulated with CoMTb.

A549 cells were incubated in hypoxia (pO₂ 1%) or pre-incubated with DMOG (0.25mM) for 2 hours and then stimulated with CoMTb. Supernatants were harvested at 72 hours and MMP-1 concentrations measured by ELISA. (A) Hypoxia significantly increases MMP-1 secretions compared to cells incubated in normoxia. (B) DMOG significantly up-regulates MMP-1 secretion compared to cells treated with DMOG or CoMTb alone. ***p<0.001